(>200, above median of overall cohort) and some degree of PD-L1 expression (weak/strong), the rate of DCB was 91% (10 of 11, 95% CI 59 to 99%). In contrast, in those with low mutation burden and some degree of PD-L1 expression, the rate of DCB was only 10% (1 of 10, 95% CI 0 to 44%). When exclusively examining patients with weak PD-L1 expression, high nonsynonymous mutation burden was associated with DCB in 75% (3 of 4, 95% CI 19 to 99%), and low mutation burden was associated with DCB in 11% (1 of 9, 0 to 48%). Large-scale studies are needed to determine the relationship between PD-L1 intensity and mutation burden. Additionally, recent data have demonstrated that the localization of PD-L1 expression within the tumor microenvironment [on infiltrating immune cells (32), at the invasive margin, tumor core, and so forth (33)] may affect the use of PD-L1 as a biomarker.

T cell recognition of cancers relies upon presentation of tumor-specific antigens on MHC molecules (34). A few preclinical (35–41) and clinical reports have demonstrated that neoantigen-specific effector T cell response can recognize (25, 42–45) and shrink established tumors (46). Our finding that nonsynonymous mutation burden more closely associates with pembrolizumab clinical benefit than total exonic mutation burden suggests the importance of neoantigens in dictating response.

The observation that anti–PD-1–induced neoantigen-specific T cell reactivity can be observed within the peripheral blood compartment may open the door to development of blood-based assays to monitor response during anti–PD-1 therapy. We believe that our findings have an important impact on our understanding of response to anti–PD-1 therapy and on the application of these agents in the clinic.

REFERENCES AND NOTES

1. W. B. Coley, Clin. Orthop. Relat. Res. 1991(262), 3–11 (1991).
2. F. S. Hodi et al., N. Engl. J. Med. 363, 711–723 (2010).
3. S. L. Topalian et al., N. Engl. J. Med. 366, 2443–2454 (2012).
4. J. D. Wolchok et al., N. Engl. J. Med. 369, 122–133 (2013).
5. C. Robert et al., Lancet 384, 1109–1117 (2014).
6. T. Powles et al., Nature 515, 558–562 (2014).
7. S. M. Ansell et al., N. Engl. J. Med. 372, 311–319 (2015).
8. E. B. Garon et al., Ann. Oncol. 25, LBA43 (2014).
9. G. P. Pfeifer, Y. H. You, A. Besaratinia, Mutat. Res. 571, 19–31 (2005).
10. G. P. Pfeifer et al., Oncogene 21, 7435–7451 (2002).
11. M. S. Lawrence et al., Nature 499, 214–218 (2013).
12. L. B. Alexandrov et al., Nature 500, 415–421 (2013).
13. B. Vogelstein et al., Science 339, 1546–1558 (2013).
14. R. Govindan et al., Cell 150, 1121–1134 (2012).
15. See supplementary text available on Science Online.
16. P. S. Hammerman et al., Nature 489, 519–525 (2012).
17. Cancer Genome Atlas Research Network, Nature 511, 543–550 (2014).
18. O. D. Abaan et al., Cancer Res. 73, 4372–4382 (2013).
19. D. Hoffmann, I. Hoffmann, K. El-Bayoumy, Chem. Res. Toxicol. 14, 767–790 (2001).
20. R. Hindges, U. Hübscher, Biol. Chem. 378, 345–362 (1997).
21. C. Palles et al., Nat. Genet. 45, 136–144 (2013).
22. J. F. Goodwin, K. E. Knudsen, Cancer Discov. 4, 1126–1139 (2014).
23. X. Wang et al., Genes Dev. 17, 965–970 (2003).
24. S. Dogan et al., Clin. Cancer Res. 18, 6169–6177 (2012).
25. A. Snyder et al., N. Engl. J. Med. 371, 2189–2199 (2014).
26. M. Nielsen et al., Protein Sci. 12, 1007–1017 (2003).
27. C. Lundegaard et al., Nucleic Acids Res. 36 (Web Server), W509–W512 (2008).
28. M. S. Rooney, S. A. Shukla, C. J. Wu, G. Getz, N. Hacohen, Cell 160, 48–61 (2015).
29. B. Rodenko et al., Nat. Protoc. 1, 1120–1132 (2006).
30. R. S. Andersen et al., Nat. Protoc. 7, 891–902 (2012).
31. J. M. Taube et al., Clin. Cancer Res. 20, 5064–5074 (2014).
32. R. S. Herbst et al., Nature 515, 563–567 (2014).
33. P. C. Tumeh et al., Nature 515, 568–571 (2014).
34. R. D. Schreiber, L. J. Old, M. J. Smyth, Science 331, 1565–1570 (2011).
35. T. Matsutake, P. K. Srivastava, Proc. Natl. Acad. Sci. U.S.A. 98, 3992–3997 (2001).
36. H. Matsushita et al., Nature 482, 400–404 (2012).
37. J. C. Castle et al., Cancer Res. 72, 1081–1091 (2012).
38. T. Schumacher et al., Nature 512, 324–327 (2014).
39. M. M. Gubin et al., Nature 515, 577–581 (2014).
40. M. Yadav et al., Nature 515, 572–576 (2014).
41. F. Duan et al., J. Exp. Med. 211, 2231–2248 (2014).
42. N. van Rooij et al., J. Clin. Oncol. 31, e439–e442 (2013).
43. P. F. Robbins et al., Nat. Med. 19, 747–752 (2013).
44. M. Rajasagi et al., Blood 124, 453–462 (2014).
45. C. Linnemann et al., Nat. Med. 21, 81–85 (2015).
46. E. Tran et al., Science 344, 641–645 (2014).

GENE EXPRESSION

MicroRNA control of protein expression noise

Jörn M. Schmiedel,[1,2,3] Sandy L. Klemm,[4] Yannan Zheng,[3] Apratim Sahay,[3] Nils Blüthgen,[1,2]*† Debora S. Marks,[5]*† Alexander van Oudenaarden[3,6,7]*†

MicroRNAs (miRNAs) repress the expression of many genes in metazoans by accelerating messenger RNA degradation and inhibiting translation, thereby reducing the level of protein. However, miRNAs only slightly reduce the mean expression of most targeted proteins, leading to speculation about their role in the variability, or noise, of protein expression. We used mathematical modeling and single-cell reporter assays to show that miRNAs, in conjunction with increased transcription, decrease protein expression noise for lowly expressed genes but increase noise for highly expressed genes. Genes that are regulated by multiple miRNAs show more-pronounced noise reduction. We estimate that hundreds of (lowly expressed) genes in mouse embryonic stem cells have reduced noise due to substantial miRNA regulation. Our findings suggest that miRNAs confer precision to protein expression and thus offer plausible explanations for the commonly observed combinatorial targeting of endogenous genes by multiple miRNAs, as well as the preferential targeting of lowly expressed genes.

MicroRNAs (miRNAs) regulate numerous genes in metazoan organisms (1–5) by accelerating mRNA degradation and inhibiting translation (6, 7). Although the physiological function of some miRNAs is known in detail (1, 2, 8, 9), it is unclear why miRNA regulation is so ubiquitous and conserved, because individual miRNAs only weakly repress the vast majority of their target genes (10, 11), and knockouts rarely show phenotypes (12). One proposed reason for this widespread regulation is the ability of miRNAs to provide precision to gene expression (13). Previous work has hypothesized that miRNAs could reduce protein expression variability (noise) when their repres-sive posttranscriptional effects are antagonized by accelerated transcriptional dynamics (14, 15). However, because miRNA levels are themselves variable, one should expect the propagation of their fluctuations to introduce additional noise (Fig. 1A).

To test the effects of endogenous miRNAs, we quantified protein levels and fluctuations in mouse embryonic stem cells (mESCs) using a dual fluorescent reporter system (16), in which two different reporters (ZsGreen and mCherry) are transcribed from a common bidirectional promoter (Fig. 1B). One of the reporters (mCherry) contained several variants and numbers of miRNA binding sites in its 3′ untranslated region (3′UTR),

and we quantified single-cell fluorescence using a flow cytometer (Fig. 1C).

We used ZsGreen fluorescence intensity to bin cells with similar transcriptional activity (mostly due to varying plasmid copy numbers) and calculated mean and noise (standard deviation divided by mean) of mCherry intensity distributions in each bin (Fig. 1D).

We first assessed the effects of endogenous miR-20a in mESCs, on a designed target site in

[1]Integrative Research Institute for the Life Sciences and Institute for Theoretical Biology, Humboldt Universität, 10115 Berlin, Germany. [2]Institute of Pathology, Charité-Universitätsmedizin, 10117 Berlin, Germany. [3]Department of Physics, Massachusetts Institute of Technology (MIT), Cambridge MA 02139, USA. [4]Department of Electrical Engineering and Computer Science, MIT, Cambridge, MA 02139, USA. [5]Department of Systems Biology, Harvard Medical School, Longwood Avenue, Boston, MA 02115, USA. [6]Department of Biology, MIT, Cambridge, MA 02139, USA. [7]Hubrecht Institute, Royal Netherlands Academy of Arts and Sciences, and University Medical Center Utrecht, Uppsalalaan 8, 3584 CT, Utrecht, Netherlands.
*Corresponding author. E-mail: nils.bluethgen@charite.de (N.B.); debbie@hms.harvard.edu (D.S.M.); a.vanoudenaarden@hubrecht.eu (A.v.O.) †These authors contributed equally to this work.

the reporter. In cells with low expression of a reporter (mCherry) containing a miR-20a site, noise was reduced (compared to an unregulated control at equal mCherry expression), in contrast to increased noise at high reporter expression (Fig. 1E). These changes in mCherry noise were more pronounced when the miR-20a sites in the reporter were perfect targets or when there were multiple sites in the 3′ UTR (Fig. 1, F and G, and fig. S1).

In order to explore the mechanism for these seemingly opposing effects on protein expression noise, we built a mathematical model where we decomposed total noise into intrinsic noise and extrinsic noise $\eta_{tot}^2 = \eta_{int}^2 + \eta_{ext}^2$ (17, 18) (see the supplementary materials). Intrinsic noise η_{int} results from the stochasticity of transcription, translation, and decay, but is mostly dominated by transcriptional dynamics (19, 20) and low mRNA copy numbers (21, 22). Extrinsic noise η_{ext} stems from fluctuations propagating from external factors to the gene (23). The modeling predicted opposing effects of miRNA regulation on intrinsic and extrinsic noise. On the one hand, the model predicted that a miRNA-regulated gene

(reg) has reduced intrinsic noise as compared to an unregulated gene (unreg) at equal protein expression levels; intrinsic noise is approximately reduced by the square root of miRNA-mediated fold repression r, $\frac{\eta_{int}^{unreg}}{\eta_{int}^{reg}} \cong \sqrt{r}$ (Fig. 2A). Noise reduction results from miRNA-mediated accelerated mRNA turnover and increased transcriptional activity needed to produce the same amount of protein (14). The model predicts that the effect occurs independently of the mode of miRNA-mediated repression (supplementary note 1). On the other hand, the model predicted that miRNA regulation acts as an additional extrinsic noise source $\eta_{ext} = \tilde{\eta}_\mu \times \varphi$ (Fig. 2B). The magnitude of η_{ext} depends on the noise in the pool of regulating miRNAs ($\tilde{\eta}_\mu$) and on how strongly miRNAs repress the target (φ) (fig. S2). Therefore, the model predicted that the combined net effects of decreased intrinsic and additional extrinsic noise would result in decreased total noise at low expression, but increased total noise at high expression (Fig. 2C); model fits, with the miRNA pool noise $\tilde{\eta}_\mu$ as the only free parameter, yield accurate agreement
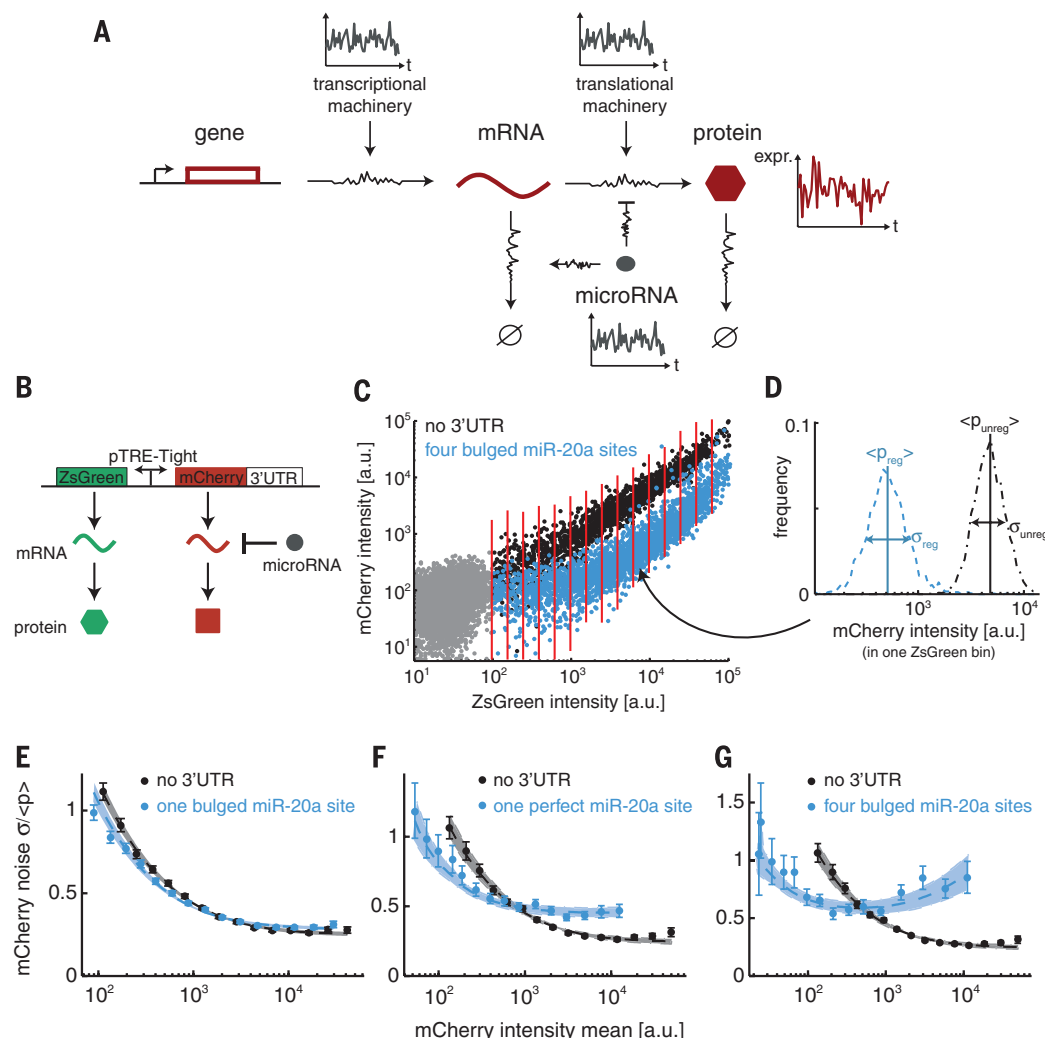

Fig. 1. miRNA regulation has opposing effects on noise at low and high protein expression. (**A**) The expression of a miRNA-regulated gene. Noise in protein expression originates from stochastic molecular reactions in the production of the protein (intrinsic noise; jagged arrows) or fluctuations propagating from external factors (extrinsic noise). (**B**) Plasmid reporter system coding for two fluorescent proteins ZsGreen and mCherry, transcribed from a common bidirectional promoter. The mCherry 3′UTR can be modified to contain miRNA binding sites. (**C**) Overlay of two flow cytometry measurements of mESC populations transiently transfected with different variants of the plasmid system: empty mCherry 3′UTR (black) and mCherry 3′UTR containing four bulged miR-20a binding sites (blue). For further processing, cells are binned according to ZsGreen intensity (red lines), and cells below ZsGreen background are discarded (gray) (supplementary materials). a.u., arbitrary units. (**D**) Mean and noise (standard deviation divided by mean σ/<p>) of mCherry intensities are calculated from marginal distributions in each bin. (**E** to **G**) Noise of mCherry intensity as a function of mean mCherry intensity in each bin for three different miR-20a–regulated constructs

(blue), as compared to respective unregulated constructs (black). Panels are ordered from left to right according to increasing repression of constructs by miR-20a (fig. S1). Dots, data; lines and shaded area, model fit.

with the experimentally observed total noise profiles (Fig. 1, E to G).

To distinguish between miRNA-mediated intrinsic and extrinsic noise effects experimentally, we modified the plasmid reporter system so that both reporters contained identical 3′UTRs (Fig. 3A and fig. S3A). Now intracellular differences in their expression can only result from processes individual to each gene (i.e., intrinsic noise). Comparing identical reporters both with and without miR-20a sites, we showed that miR-20a regulation reduced intrinsic noise, as compared to an unregulated construct (Fig. 3B), by the square root of fold repression, as predicted by modeling (Fig. 3C and fig. S3D). These results also show that the observed increase in total noise at high mCherry expression must be due to additional extrinsic noise (fig. S3C).

The model and the experiments suggest that the reduction of intrinsic noise is a generic property of miRNAs and should occur irrespective of the specific miRNAs or the molecular details of the mRNA-miRNA interaction. To test the generality of these conclusions, we constructed eight additional reporters with mCherry 3′UTRs containing a perfect binding site for a variety of miRNAs that are endogenously expressed in mESCs (fig. S4). For all constructs, the intrinsic noise reduction was approximately the square root of fold repression (using model fit to total noise, figs. S3E and S5). This was also confirmed by direct measurement for miR-291a target sites (Fig. 3C and fig. S3B) and reporters containing AU-rich elements (24) (figs. S3F and S6), the latter further supporting the plausibility that the

reduction of intrinsic noise is a generic property of posttranscriptional repressors.

Additional extrinsic noise stems from the variability of the miRNA pool, and consistent with this, we find that miRNA pool noise indeed differs between miRNAs (Fig. 3D). The validity of these results is supported by the observation that different constructs assaying the same miRNA yield similar pool noise estimates (fig. S7). Although miRNA pool noise decreases for miRNAs conferring stronger repression, it is still substantial for the most potent and highly expressed miRNAs in mESCs [miR-290 cluster (25)] (Fig. 3D). The miRNAs with two independent gene copies, producing the identical mature miRNA (Fig. 3D, red), tend to have lower miRNA pool noise than to single-gene miRNAs. This suggested to us that
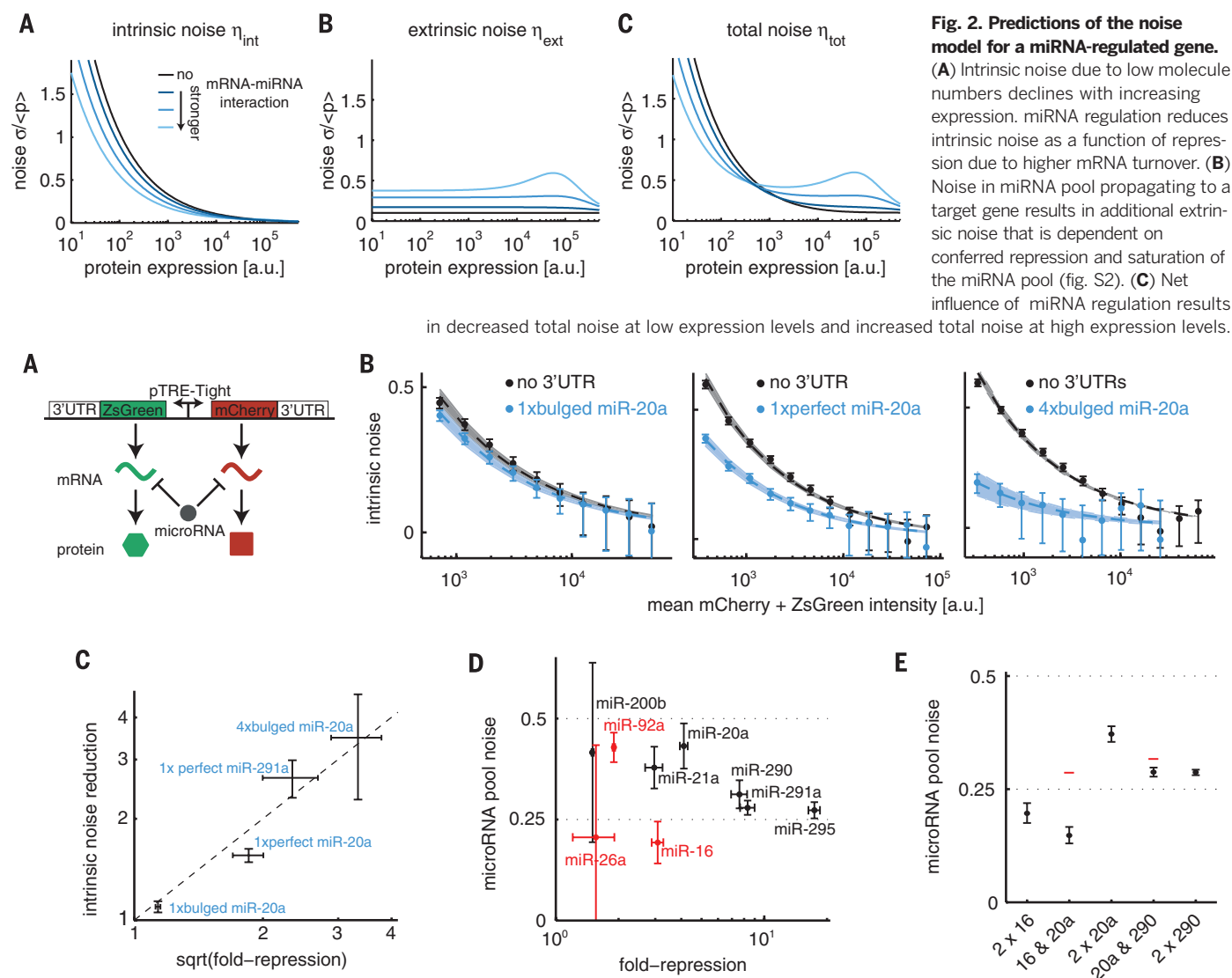

Fig. 2. Predictions of the noise model for a miRNA-regulated gene. (**A**) Intrinsic noise due to low molecule numbers declines with increasing expression. miRNA regulation reduces intrinsic noise as a function of repression due to higher mRNA turnover. (**B**) Noise in miRNA pool propagating to a target gene results in additional extrinsic noise that is dependent on conferred repression and saturation of the miRNA pool (fig. S2). (**C**) Net influence of miRNA regulation results in decreased total noise at low expression levels and increased total noise at high expression levels.

Fig. 3. Exploration of intrinsic and extrinsic noise effects. (**A**) Plasmid reporter system with identical 3′UTRs for ZsGreen and mCherry, to quantify expression-dependent intrinsic noise. (**B**) Intrinsic noise as a function of expression for three different miR-20a biregulated constructs. Dots, data; lines and shaded area, model fit. (**C**) Measured intrinsic noise reduction for biregulated constructs compared to fold repression, as measured independently by mCherry-regulated constructs (fig. S1). *n* = 3 biological replicates. (**D**) miRNA pool noise estimates for nine different miRNAs endogenously expressed in mESCs. A subset of miRNAs with two instead of one gene copies is indicated in red; *n* ≥ 3 biological replicates. (**E**) miRNA pool noise estimates for individual and mixed pools, using data from reporters with two perfect binding sites behind mCherry as indicated. Red bars, expectation for mixed pool noise when subpools were fully correlated. *n* = 3 biological replicates.

miRNA pools could have lower noise if they consist of independently transcribed miRNAs, and thus uncorrelated fluctuations can average out. To test this hypothesis, we constructed reporters with perfect target sites for miR-20a and either miR-16 or miR-290 in the mCherry 3′UTR and compared them to reporters with two perfect target sites for miR-16, miR-20a, or miR-290, respectively. We found that the noise levels in the mixed pools were lower than expected if the individual miRNA pools were fully correlated and could be lower than the noise in the individual miRNA pools (Fig. 3E and fig. S8). Therefore, our data show that, if noise between different miRNAs is not correlated, combinatorial regulation can result in lower noise of the target protein.

In contrast to our artificial 3′UTRs, endogenous mRNAs often contain many binding sites to different miRNAs and with less complementarity (3, 26). To test whether our findings are likely to be applicable in vivo, we constructed mCherry reporters with the 3′UTRs from *Wee1*, *Lats2, Casp2*, and *Rbl2*, all predicted to be com-

binatorial regulated by mESC miRNAs (table S1). This multiple-miRNAs regulation resulted in 3- to 5.5-fold repression as compared to the control 3′UTRs containing mutated sites (fig. S9A) and reduced total noise except when reporter expression levels were high (Fig. 4A and fig. S9A). Model fits estimate intrinsic noise reduction for the wild-type 3′UTRs as large as the square root of fold repression (fig. S3G), consistent with our findings for the artificial 3′UTRs. Furthermore, little additional noise at high expression levels results from low noise in the mixed miRNA pools regulating the wild-type 3′UTRs (fig. S9B), corroborating the idea that combinatorial miRNA regulation is a potent way to optimize overall noise reduction.

To determine whether the reporter assay covers expression levels relevant to endogenous genes, we used fluorescence-activated cell sorting (FACS) and RNA sequencing (fig. S10A). The reporter assay covers the range of 25 to 99% of expressed genes in mESCs (Fig. 4B). Model-based extrapolation shows that the reduction of total noise for the endogenous 3′UTRs extends in a graded

fashion up to the top 10% of the transcriptome expression distribution (Fig. 4C). Although most miRNAs individually repress genes only to a small extent (10, 11), hundreds of genes are substantially repressed (>twofold) by the combinatorial action of miRNAs in mESCs (fig. S11), as determined from transcriptome expression data for wild-type and miRNA-deficient Dicer knockout mESCs (27). Furthermore, most of the highly repressed genes have low expression levels [fig. S11, consistent with (28, 29)], suggesting that these genes should have reduced protein expression noise as a consequence of miRNA regulation in vivo.

Our integrated theoretical and experimental analyses show that the reduction of intrinsic noise is a generic property of miRNA regulation (and more generally posttranscriptional regulation) that is linked to the repression of protein expression. miRNAs preferentially target lowly expressed genes, for which noise reduction will be strongest, while selectively avoiding ubiquitous and highly expressed genes (28, 29). Combinatorial miRNA regulation, a widely observed phenomenon in vivo (3, 26), enhances overall noise reduction by providing strong repression to endogenous genes with only little additional noise from miRNA pools. Combinatorial miRNA regulation may thus be a potent mechanism to reinforce cellular identity by reducing gene expression fluctuations that are undesirable for the cell.
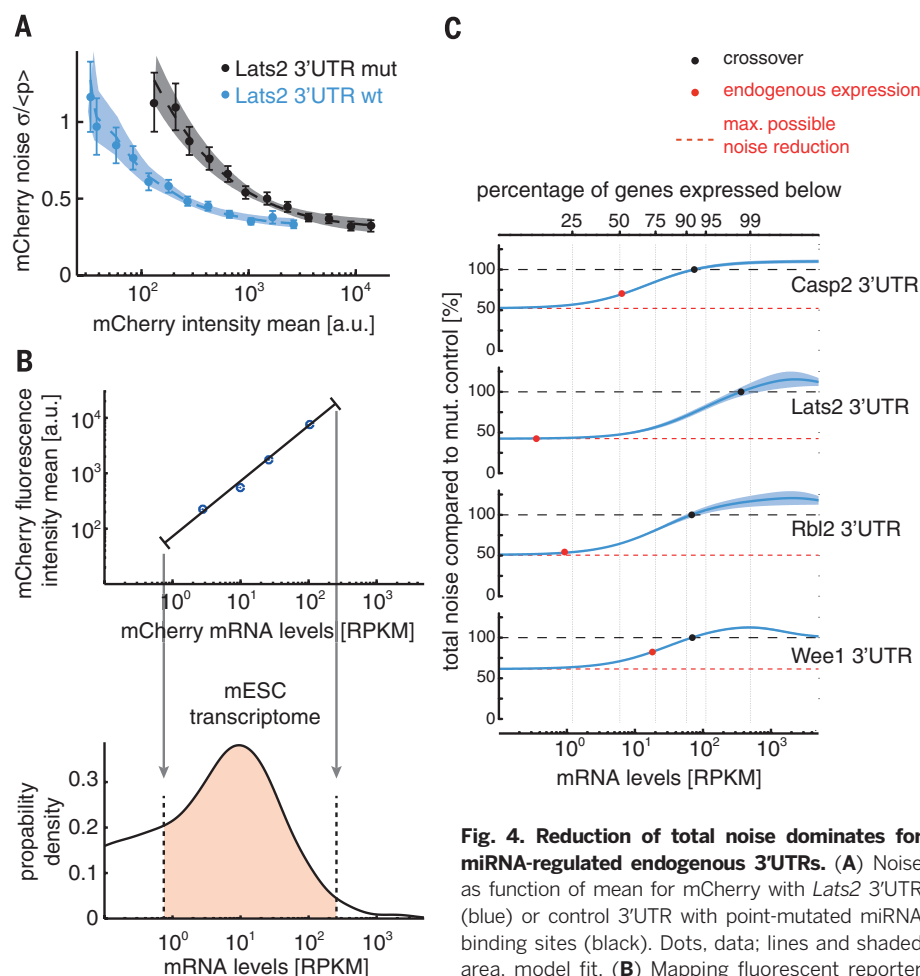

Fig. 4. Reduction of total noise dominates for miRNA-regulated endogenous 3′UTRs. (**A**) Noise as function of mean for mCherry with *Lats2* 3′UTR (blue) or control 3′UTR with point-mutated miRNA binding sites (black). Dots, data; lines and shaded area, model fit. (**B**) Mapping fluorescent reporter range to mESC transcriptome. (Upper panel) FACS and least-squares regression were used to determine conversion between mean mCherry fluorescent intensities and mCherry mRNA levels (as measured by RNA-seq). (Lower panel) Range covered by mCherry in relation to transcriptome expression in mESCs (~25 to ~99%). FPKM, fragments per kilobase of exon model per million mapped reads. (**C**) Model-based extrapolation of total noise in assayed endogenous 3′UTRs relative to control 3′UTRs as a function of transcriptome expression (blue line and area, mean and 95% confidence interval based on parameter estimates of three biological replicates).

REFERENCES AND NOTES

1. R. C. Lee, R. L. Feinbaum, V. Ambros, *Cell* **75**, 843–854 (1993).
2. B. Wightman, I. Ha, G. Ruvkun, *Cell* **75**, 855–862 (1993).
3. A. J. Enright *et al.*, *Genome Biol.* **5**, R1 (2003).
4. B. John *et al.*, *PLOS Biol.* **2**, e363 (2004).
5. B. P. Lewis, C. B. Burge, D. P. Bartel, *Cell* **120**, 15–20 (2005).
6. H. Guo, N. T. Ingolia, J. S. Weissman, D. P. Bartel, *Nature* **466**, 835–840 (2010).
7. L. P. Lim *et al.*, *Nature* **433**, 769–773 (2005).
8. J. Brennecke, D. R. Hipfner, A. Stark, R. B. Russell, S. M. Cohen, *Cell* **113**, 25–36 (2003).
9. R. J. Johnston Jr., O. Hobert, *Nature* **426**, 845–849 (2003).
10. D. Baek *et al.*, *Nature* **455**, 64–71 (2008).
11. M. Selbach *et al.*, *Nature* **455**, 58–63 (2008).
12. E. A. Miska *et al.*, *PLOS Genet.* **3**, e215 (2007).
13. D. P. Bartel, C.-Z. Chen, *Nat. Rev. Genet.* **5**, 396–400 (2004).
14. M. S. Ebert, P. A. Sharp, *Cell* **149**, 515–524 (2012).
15. J. Noorbakhsh, A. H. Lang, P. Mehta, *PLOS ONE* **8**, e72676 (2013).
16. S. Mukherji *et al.*, *Nat. Genet.* **43**, 854–859 (2011).
17. M. B. Elowitz, A. J. Levine, E. D. Siggia, P. S. Swain, *Science* **297**, 1183–1186 (2002).
18. P. S. Swain, M. B. Elowitz, E. D. Siggia, *Proc. Natl. Acad. Sci. U.S.A.* **99**, 12795–12800 (2002).
19. W. J. Blake, M. KÆrn, C. R. Cantor, J. J. Collins, *Nature* **422**, 633–637 (2003).
20. A. Raj, C. S. Peskin, D. Tranchina, D. Y. Vargas, S. Tyagi, *PLOS Biol.* **4**, e309 (2006).
21. E. M. Ozbudak, M. Thattai, I. Kurtser, A. D. Grossman, A. van Oudenaarden, *Nat. Genet.* **31**, 69–73 (2002).
22. A. Bar-Even *et al.*, *Nat. Genet.* **38**, 636–643 (2006).
23. J. M. Pedraza, A. van Oudenaarden, *Science* **307**, 1965–1969 (2005).
24. C. Barreau, L. Paillard, H. B. Osborne, *Nucleic Acids Res.* **33**, 7138–7150 (2005).
25. A. Marson *et al.*, *Cell* **134**, 521–533 (2008).
26. A. Krek *et al.*, *Nat. Genet.* **37**, 495–500 (2005).
27. A. K. L. Leung *et al.*, *Nat. Struct. Mol. Biol.* **18**, 237–244 (2011).
28. P. Sood, A. Krek, M. Zavolan, G. Macino, N. Rajewsky, *Proc. Natl. Acad. Sci. U.S.A.* **103**, 2746–2751 (2006).
29. K. K.-H. Farh *et al.*, *Science* **310**, 1817–1821 (2005).

EPIGENETICS

Restricted epigenetic inheritance of H3K9 methylation

Pauline N. C. B. Audergon, Sandra Catania,* Alexander Kagansky,† Pin Tong,
Manu Shukla, Alison L. Pidoux, Robin C. Allshire‡

Posttranslational histone modifications are believed to allow the epigenetic transmission of distinct chromatin states, independently of associated DNA sequences. Histone H3 lysine 9 (H3K9) methylation is essential for heterochromatin formation; however, a demonstration of its epigenetic heritability is lacking. Fission yeast has a single H3K9 methyltransferase, Clr4, that directs all H3K9 methylation and heterochromatin. Using releasable tethered Clr4 reveals that an active process rapidly erases H3K9 methylation from tethering sites in wild-type cells. However, inactivation of the putative histone demethylase Epe1 allows H3K9 methylation and silent chromatin maintenance at the tethering site through many mitotic divisions, and transgenerationally through meiosis, after release of tethered Clr4. Thus, H3K9 methylation is a heritable epigenetic mark whose transmission is usually countered by its active removal, which prevents the unauthorized inheritance of heterochromatin.

I n most eukaryotes, the methylation of nucleosomal histone H3 on lysine 9 (H3K9me) is required for the assembly of constitutive heterochromatin (1). H3K9me2/3 is bound by HP1/Swi6 proteins and Suv39/Clr4 H3K9 methyltransferases to form heterochromatic regions (2–6). Because Suv39 and Clr4 can bind the H3K9me2/3 marks that they generate, and because HP1 proteins may also facilitate recrui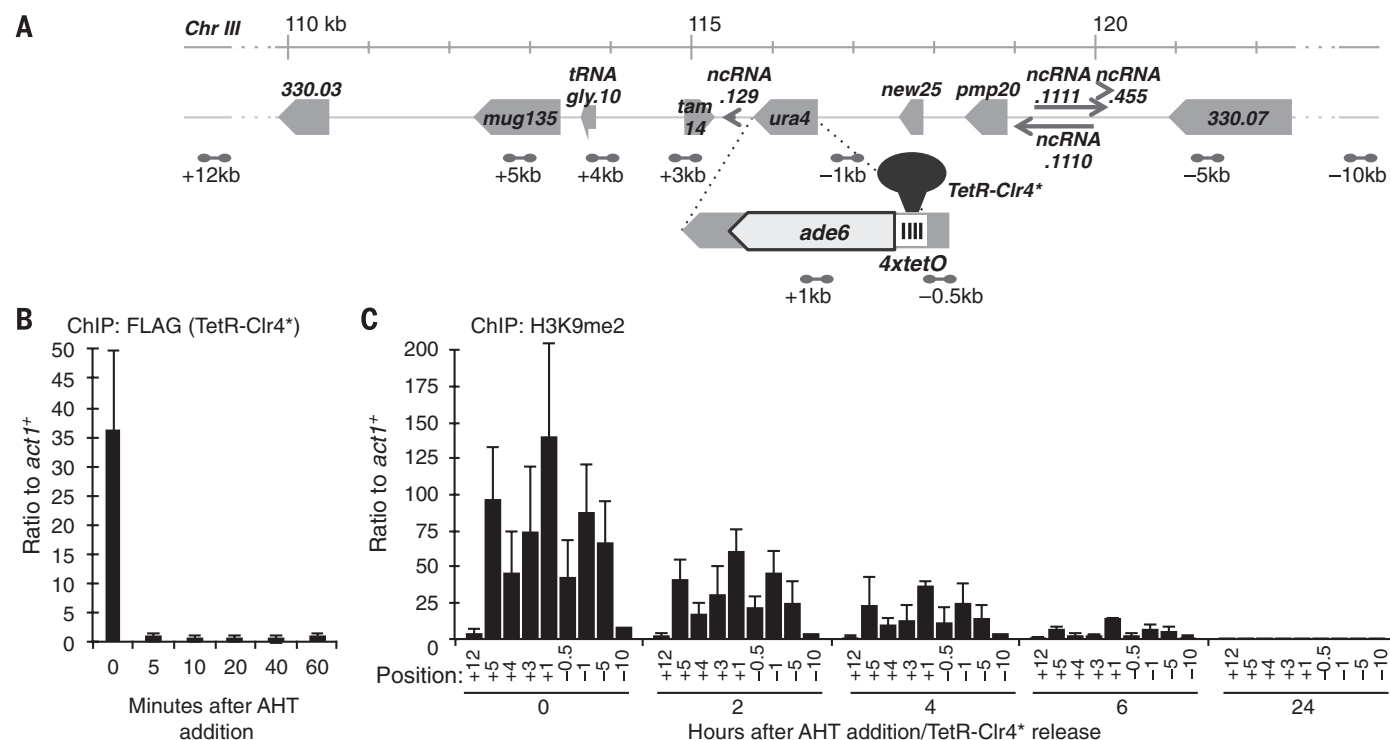tment of these methyltransferases (7), it is thought that H3K9 methylation and heterochromatin can be maintained by self-propagation, even when the initiator is withdrawn (8, 9). However, in eukaryotic systems that exhibit overtly heritable chromatin states, there is often a tight relationship between DNA methylation, H3K9 methylation, and heterochromatin, confounding analyses of the heritability of H3K9 methylation (10, 11). Fission yeast lacks DNA methylation and a single nonessential methyltransferase, Clr4 (Suv39 ortholog), is responsible for all H3K9me-dependent heterochromatin (12). Thus, fission yeast is an ideal system in which to determine whether H3K9me-dependent heterochromatin is truly heritable. Clr4 normally requires sequence-directed targeting to particular chromosomal regions via RNA interference (RNAi) in a process involving

Wellcome Trust Centre for Cell Biology and Institute of Cell Biology, School of Biological Sciences, The University of Edinburgh, Max Born Crescent, Edinburgh EH9 3BF, Scotland, UK.
*Present address: Department of Biochemistry and Biophysics, University of California, San Francisco, CA 94158, USA. †Present address: Medical Research Council (MRC) Human Genetics Unit, MRC Institute of Genetics and Molecular Medicine, The University of Edinburgh, Edinburgh EH4 2XU, Scotland, UK. ‡Corresponding author. E-mail: robin.allshire@ed.ac.uk

Fig. 1. H3K9 methylation is rapidly lost upon release of tethered TetR-Clr4*. (**A**) Positions of *4xtetO*, tethered TetR-Clr4* beside *ade6⁺* at *ura4*, and surrounding *Schizosaccharomyces pombe* chromosome III genes. Dumbbells indicate primer pairs. ncRNA, noncoding RNA. (**B** and **C**) Quantitative chromatin immunoprecipitation (qChIP) time course of FLAG-TetR-Clr4* (B) and H3K9me2 (C) levels on *4xtetO-ade6⁺* after AHT addition using the indicated primers. Data are mean ± SD (error bars) (*n* = 3 experimental replicates). *P* < 0.05 (*t* test).